28 May 2016 Volume 144 Number 20

AIP | The Journal of Chemical Physics

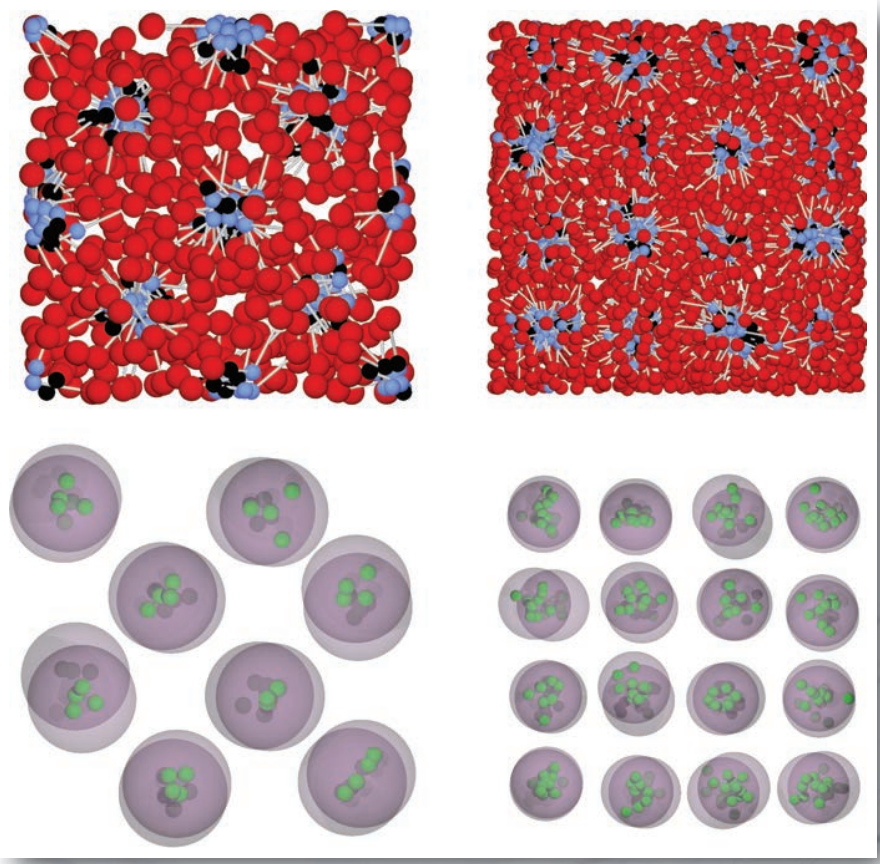

jcp.aip.org

AIP | The Journal of Chemical Physics

Thermodynamic stability and structural properties of cluster crystals formed by amphiphilic dendrimers

Dominic A. Lenz, Bianca M. Mladek, Christos N. Likos, and Ronald Blaak

Citation: The Journal of Chemical Physics **144**, 204901 (2016); doi: 10.1063/1.4950953
View online: http://dx.doi.org/10.1063/1.4950953
View Table of Contents: http://scitation.aip.org/content/aip/journal/jcp/144/20?ver=pdfcov
Published by the AIP Publishing

Articles you may be interested in

The electronic structure, mechanical and thermodynamic properties of Mo2XB2 and MoX2B4 (X=Fe, Co, Ni) ternary borides
J. Appl. Phys. **118**, 075902 (2015); 10.1063/1.4928628

Theoretical calculations for structural, elastic, and thermodynamic properties of RuN2 under high pressure
J. Appl. Phys. **116**, 053511 (2014); 10.1063/1.4891823

Molecular dynamics study of structure H clathrate hydrates of methane and large guest molecules
J. Chem. Phys. **128**, 194505 (2008); 10.1063/1.2908074

Thermodynamical and structural properties of imidazolium based ionic liquids from molecular simulation
J. Chem. Phys. **128**, 154509 (2008); 10.1063/1.2907332

An International Standard Formulation for the Thermodynamic Properties of 1,1,1-Trifluoroethane (HFC-143a) for Temperatures From 161 to 450 K and Pressures to 50 MPa
J. Phys. Chem. Ref. Data **29**, 521 (2000); 10.1063/1.1318909

Reuse of AIP Publishing content is subject to the terms: https://publishing.aip.org/authors/rights-and-permissions. Downloaded to IP: 91.115.166.109 On: Mon, 23 May 2016 16:29:26

THE JOURNAL OF CHEMICAL PHYSICS **144**, 204901 (2016)

Thermodynamic stability and structural properties of cluster crystals formed by amphiphilic dendrimers

Dominic A. Lenz,[1] Bianca M. Mladek,[2] Christos N. Likos,[1] and Ronald Blaak[1]
[1]*Faculty of Physics, University of Vienna, Boltzmanngasse 5, A-1090 Vienna, Austria*
[2]*Department of Structural and Computational Biology, Max F. Perutz Laboratories GmbH, University of Vienna, Campus Vienna Biocenter 5, A-1030 Vienna, Austria*

(Received 23 March 2016; accepted 4 May 2016; published online 23 May 2016)

We pursue the goal of finding real-world examples of macromolecular aggregates that form cluster crystals, which have been predicted on the basis of coarse-grained, ultrasoft pair potentials belonging to a particular mathematical class [B. M. Mladek *et al.*, Phys. Rev. Lett. **46**, 045701 (2006)]. For this purpose, we examine in detail the phase behavior and structural properties of model amphiphilic dendrimers of the second generation by means of monomer-resolved computer simulations. On augmenting the density of these systems, a fluid comprised of clusters that contain several overlapping and penetrating macromolecules is spontaneously formed. Upon further compression of the system, a transition to multi-occupancy crystals takes place, the thermodynamic stability of which is demonstrated by means of free-energy calculations, and where the FCC is preferred over the BCC-phase. Contrary to predictions for coarse-grained theoretical models in which the particles interact exclusively by effective *pair* potentials, the internal degrees of freedom of these molecules cause the lattice constant to be density-dependent. Furthermore, the mechanical stability of monodisperse BCC and FCC cluster crystals is restricted to a bounded region in the plane of cluster occupation number versus density. The structural properties of the dendrimers in the dense crystals, including their overall sizes and the distribution of monomers are also thoroughly analyzed. *Published by AIP Publishing.* [http://dx.doi.org/10.1063/1.4950953]

I. INTRODUCTION

The formation of stable clusters crystals,[1] i.e., crystals with multiply occupied lattice sites of overlapping particles, is a well-established property for soft spheres with a particular type of interaction, and it has been the subject of intensive theoretical investigations since their first discovery a few years ago.[2–10] Whereas early work had mainly focused on the behavior of simplified mathematical models,[11–17] it has been later demonstrated that the infinite-dilution effective interaction between suitably designed macromolecules fulfills the criteria set forth for the formation of cluster crystals,[18,19] thus bringing the latter into the realm of what is realizable experimentally. This kind of organization in complex fluids provides a vast richness of fascinating and highly unusual properties. Among these are intriguing phase[2] and compression behavior,[20] unusual dynamics, phonon spectra and isostructural transitions at low temperatures,[10,21,22] lattice-site to lattice-site particle exchange, i.e., hopping,[23,24] as well as the finding that such systems are non-Newtonian fluids with unique rheology and transport behavior.[25,26]

The main criterion necessary to be satisfied by particles to feature the ability to form cluster crystals was put forward by Likos *et al.*[19] and lies in the characteristic behavior of the Fourier transformation $\hat{\phi}(q)$ of the particle pair-interaction $\phi(r)$, where r is the separation between the particles and q is a wavenumber in reciprocal space. The criterion applies to interactions that decay to zero sufficiently fast at large distances and are bounded for all separations r, so that the potential is integrable and the Fourier transformation exists. The criterion establishes that only two possible scenarios for the system behavior exist, depending solely on the sign of $\hat{\phi}(q)$. If $\hat{\phi}(q)$ is a non-negative function, i.e., $\hat{\phi}(q) \geq 0$ for all q-values, the system will show re-entrant melting behavior at high densities. More precisely, at sufficiently low temperature there is a low-density phase transition from a fluid to a crystal with single occupied lattice sites, but at high temperatures a fluid is the only stable phase at all densities.[27,28] Accordingly, at low temperatures there must be a reentrant melting transition on the high density-side, and the system displays a maximal freezing temperature as well. This type of potential belongs to the so-called Q^+ class of functions. If, on the other hand, the potential $\hat{\phi}(q)$ attains negative values for certain ranges of the wavenumber q, it is categorized as belonging to the $Q^\pm$ class of functions. For such systems, the fluid state is absolutely unstable at all temperatures for sufficiently high densities,[19,29,30] leading to the formation of cluster crystals. It should be emphasized that attractions are not necessary; even purely repulsive interactions lead to cluster formation, as long as they belong to the $Q^\pm$-class.[18,20,29] A typical and well studied example for such potentials are the members of the generalized exponential model (GEM), which have the form $\phi(r) = \epsilon \exp[-(r/\sigma)^n]$, ϵ and σ being the energy and the length scales of the interaction, respectively. The transition between Q^+ and $Q^\pm$ for this special class of potentials lies exactly at $n = 2$ corresponding to the Gaussian core model.[29] The penetrable sphere model[11–17] is obtained as the limiting case of the GEM-model for $n \to \infty$.

Reuse of AIP Publishing content is subject to the terms: https://publishing.aip.org/authors/rights-and-permissions. Downloaded to IP: 91.115.166.109 On: Mon, 23 May 2016 16:29:26

To proceed from a mathematical to a physically motivated model, one has to address the question of how such systems could be experimentally realizable: after all, the usual, atomistic or molecular interaction potentials are diverging at small separations whereas the aforementioned effective ones remain bounded, raising the issue of whether the effective interactions can be physical. If one considers, however, polymeric macromolecules, one finds that a bounded potential can be understood in terms of an *effective* pair-interaction[20,31–36] acting between suitably chosen, coarse-grained degrees of freedom. In the process of obtaining this effective description, the full set of internal degrees of freedom of the monomeric units is integrated out and replaced by a small number of degrees of freedom. The simplest and most popular choice is to replace each molecule with its center of mass and to integrate out all orientations, so that an effective pair potential $\phi(r) = \phi_{\text{eff}}(r)$ between any two centers of mass results, which only depends on the relative distance r between them.[32,37] Such effective interactions for macromolecular systems and low monomer concentrations are in general bounded, since centers of mass are not material particles and thus they can fully overlap paying only a finite free energy penalty.

There is a caveat with the aforementioned approach: the effective pair-potential is actually density-dependent due to the fact that the statistics of the internal degrees of freedom of flexible macromolecules is, in general, dependent on concentration. In the theoretical description, one employs instead a density-independent interaction for all concentrations, which is derived by considering just two interacting molecules in a large volume, i.e., in the infinite-dilution limit. It is tempting to use this approach, at least as a first-order approximation, assuming that the effective interaction is not markedly affected by the density, and postulating thus its validity also for the higher densities in which cluster crystals form. It is not *a priori* clear, though, how reliable such an approximation is. A good illustration of a system where the approach based on the infinite-dilution effective interaction fails is a system of ring polymers. The effective pair-interaction for rings is indeed of the $Q^{\pm}$ type in the zero density limit, but full monomer-resolved simulations of these systems reveal no hint of clustering at higher densities.[34] In this particular case, this is caused by the fact that beyond the overlap concentration, the rings undergo very substantial deformations in comparison to their shapes and conformations at infinite dilution. Accordingly, the full effective Hamiltonian would include many-body terms, which are expressed as a strongly density-dependent effective pair potential. The finite-density effective pair potential differs dramatically from its infinite-dilution counterpart, thus the predictions based on the latter turn out to be unreliable. More sophisticated approaches than a reduction to the center of mass are thus called upon to properly coarse-grain concentrated ring-polymer solutions.[38]

A different candidate system for the formation of cluster crystals was proposed by Mladek *et al.*[18] in the form of second generation amphiphilic dendrimers, for which the effective pair-interaction also belongs to the $Q^{\pm}$ class of potentials. For this system, the clustering phenomenon extends to higher densities and gives rise to a cluster fluid,[7] also showing indications of forming stable cluster crystals. The structure of such a conjectured crystal is schematically illustrated in Fig. 1 and entails three levels. At the microscopic level, we find the monomeric description of the dendrimers that at the coarse grained level are represented by a soft spherical object. On increasing the density, a number of these dendrimers are expected to form a cluster of overlapping particles. The clusters can be thought of as a new structural unit at the next step of coarse graining that form a crystal on the third structural level. The existence of cluster crystals in these model dendrimer systems was demonstrated explicitly by means of monomer-resolved computer simulations and their thermodynamical stability was confirmed by free energy calculations.[39] Here we will examine various aspects of those results in more detail and we investigate in detail the internal structure of clusters and crystals.

The rest of this work is organized as follows: we give a detailed description of the dendrimer model in Sec. II. In Sec. III we recapitulate the main constituents of the theoretical framework employed to describe the formation of cluster crystals in the effective potential picture and discuss its predictions for the system at hand. Monomer-resolved computer simulation results for the cluster fluid phase are shown in Sec. IV. In Sec. V we analyze the mechanical

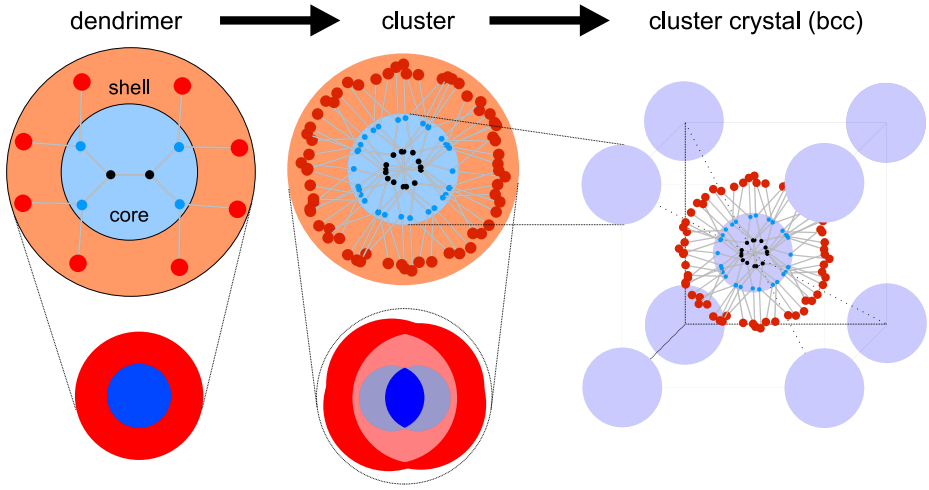

FIG. 1. Schematic representations of the primary internal structure of a single amphiphilic dendrimer of second generation (left), the secondary structure in which dendrimers pack into clusters (middle), and the tertiary structure of the formation of a BCC cluster crystal (right). The two lower images represent a coarse grained description of a dendrimer and a cluster. The core and shell monomers/shells are represented by blue (black) and red spheres/regions, respectively.

Reuse of AIP Publishing content is subject to the terms: https://publishing.aip.org/authors/rights-and-permissions. Downloaded to IP: 91.115.166.109 On: Mon, 23 May 2016 16:29:26

stability of the cluster crystals that have been investigated, whereas in Sec. VI we examine the internal structure of clusters in these crystals. The thermodynamic stability of cluster crystals is addressed in Sec. VII by means of free energy calculations. Finally, in Sec. VIII we summarize and draw our conclusions.

II. DENDRIMER MODELS AND MAIN PROPERTIES

For our computer simulations we employ a simple model for second generation amphiphilic dendrimers that was introduced by Mladek *et al.*[7,18,40,41] Each dendrimer, an example of which schematically is shown in Fig. 1, is formed by a central pair of generation $g = 0$ monomers and to either of them, two generation $g = 1$ monomers are attached. Together these six monomers form the solvophobic core of the dendrimer, which is surrounded by a solvophilic shell formed by a total of eight monomeric units of generation $g = 2$. The latter are evenly distributed by connecting them in pairs to each of the $g = 1$ core monomers. In this fashion, a small amphiphilic dendrimer consisting of just 14 monomers is formed. In order to distinguish the two types of monomers we introduce the sub-indices C and S for the core and shell monomers, respectively.

Intra- and inter-molecular interactions between any two monomers, separated by a distance r, are modeled by the Morse potential[42]

$$\beta\Phi_{\mu\nu}^{\mathrm{Morse}}(r) = \epsilon_{\mu\nu}\left\{\left[e^{-\alpha_{\mu\nu}(r-\sigma_{\mu\nu})} - 1\right]^2 - 1\right\}, \quad \mu\nu = \mathrm{CC, CS, SS} \tag{1}$$

where $\sigma_{\mu\nu}$ denotes the effective diameter between two monomers of species μ and ν, with $\mu, \nu = \mathrm{C}$ or S. The potentials are measured in terms of the inverse temperature $\beta = (k_{\mathrm{B}}T)^{-1}$, with k_{B} the Boltzmann constant. The Morse potential is characterized by a repulsive short-range behavior and an attractive part at long distances, whose range and depth are parameterized via $\alpha_{\mu\nu}$ and $\epsilon_{\mu\nu}$, respectively. By choosing appropriate values for these parameters, the solvent-mediated interactions result in the solvophobic and solvophilic character observed for amphiphilic dendrimers.

The connectivity within the dendrimers is maintained by the finitely extensible nonlinear elastic (FENE) potential, given by

$$\beta\Phi_{\mu\nu}^{\mathrm{FENE}}(r) = -K_{\mu\nu}R_{\mu\nu}^2 \log\left[1 - \left(\frac{r - l_{\mu\nu}}{R_{\mu\nu}}\right)^2\right], \quad \mu\nu = \mathrm{CC, CS} \tag{2}$$

where the spring constant $K_{\mu\nu}$ restricts the monomer separation r to be within a distance $R_{\mu\nu}$ from the equilibrium bond length $l_{\mu\nu}$.

We will be employing two different sets of interaction parameters, denoted by Model I and Model II, as listed in Table I. Model I corresponds to the amphiphilic dendrimers that were introduced by Mladek *et al.*[7,18,40,41] Model II was introduced more recently by Lenz *et al.*[39] and it facilitates the formation of thermodynamically stable cluster crystals with a lower cluster occupancy, which makes this behavior more easily accessible by means of computer simulations. This is achieved by a combination of an equilibrium bond length between the two central monomers that is larger then the bond-length between 0th and 1st generation monomers, a wider range of attraction between core monomers, and a larger size of the shell monomers. The effective size $\sigma \equiv \sigma_{\mathrm{CC}}$ of the core monomers, which is the same for both models, will be the unit of length.

The size of the two model dendrimers at infinite dilution as determined by computer simulation is $R_g^{\mathrm{I}} = 3.36\sigma$ and $R_g^{\mathrm{II}} = 3.58\sigma$, $R_g^{\mathrm{I,II}}$ denoting the radius of gyration for Model I and Model II, respectively. The latter is slightly larger due to the increased equilibrium bond-length between the two central core monomers. More important with respect to the phase behavior of these systems, however, are the effective pair-interactions between the centers of mass, shown in Fig. 2.[43] They can be obtained from the simulation of two isolated dendrimers on the monomeric level in combination with the umbrella sampling technique.[7,18] The shape of this interaction for the two models is similar. At large separations, where the regions of repulsive, solvophilic shells of the two dendrimers are partially overlapping, the effective interaction is correspondingly repulsive. Upon closer approach, also the core regions start to overlap. The solvophobic core monomers experience a relatively strong mutual attractive interaction that counteracts the long-range repulsion stemming from the SS- and CS-interactions. As a result of the combined effects, for

TABLE I. The interaction parameters used in Model I and Model II for the Morse interaction, Eq. (1), and the FENE bonds, Eq. (2). The labels C and S correspond to core and shell monomers, respectively.

	Model I			Model II		
Morse	$\epsilon_{\mu\nu}$	$\alpha_{\mu\nu}\sigma$	$\sigma_{\mu\nu}/\sigma$	$\epsilon_{\mu\nu}$	$\alpha_{\mu\nu}\sigma$	$\sigma_{\mu\nu}/\sigma$
CC	0.714	6.4	1.0	0.714	1.8	1.0
CS	0.014 28	19.2	1.25	0.017 85	6.0	1.75
SS	0.014 28	19.2	1.5	0.017 85	6.0	2.5
FENE	$K_{\mu\nu}\sigma^2$	$l_{\mu\nu}/\sigma$	$R_{\mu\nu}/\sigma$	$K_{\mu\nu}\sigma^2$	$l_{\mu\nu}/\sigma$	$R_{\mu\nu}/\sigma$
CC (g = 0)	40	1.875	0.375	60	3.1875	0.6375
CC	40	1.875	0.375	60	1.875	0.375
CS	20	3.75	0.75	30	3.5625	0.7125

Reuse of AIP Publishing content is subject to the terms: https://publishing.aip.org/authors/rights-and-permissions. Downloaded to IP: 91.115.166.109 On: Mon, 23 May 2016 16:29:26

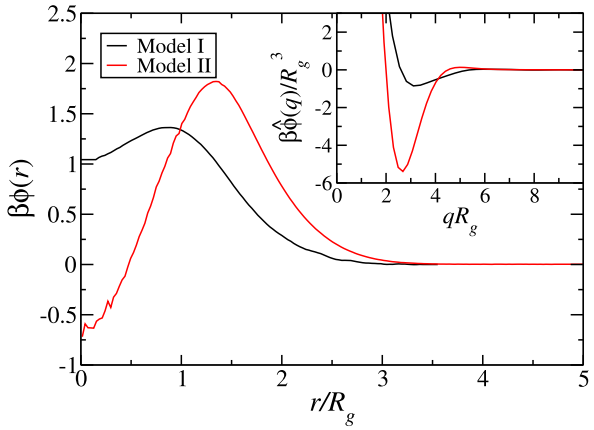

FIG. 2. The effective pair interaction $\phi(r)$ between two amphiphilic dendrimers for both models. The inset shows the corresponding Fourier transforms $\hat{\phi}(q)$.

a center of mass distance of less than a radius of gyration, an effective attraction between the two dendrimers develops.

The effective interaction resulting from Model II features a significantly stronger attraction between the dendrimers at short range and provides an intuitive argument to explain the increased thermodynamic stability for the formation of cluster crystals (see also Section III that follows). At the same time, the *negative* minimum that it has for $r = 0$ renders this pair potential *unstable*, in the sense that a many-body system of point particles interacting pairwise by this potential would lack a thermodynamic limit, featuring instead collapse of infinitely many particles onto a finite droplet.[44] This is, however, no reason for concern: the effective pair interaction is employed here only as an intermediate tool within the framework of a mean-field approximation (MFA) in which the aforementioned instability is suppressed. The MFA allows us to obtain a ball-park prediction on the density-region in which cluster formation can be expected. All subsequent investigations are carried through by means of the original, microscopic interactions, all of which feature strong short-range steric repulsions between monomers and are thus free of any pathologies. The quantitative reliability of the MFA on the basis of the effective interaction is then established *a posteriori*.

III. MEAN-FIELD APPROXIMATION FOR THE EFFECTIVE INTERACTIONS

The overall shapes of the effective pair-interactions $\phi(r)$ between dendrimers for both models, shown in Fig. 2, classify them as members of the class of $Q^{\pm}$-potentials.[19] For such bounded interactions, as well as for their Q^{+}-counterparts,[28,45] the MFA has been shown to be extremely accurate in predicting the structure of the fluid phase as well as the formation of the clusters and the instability of the fluid that leads to the cluster crystal formation.[19,29] In what follows, we recapitulate the predictions from the MFA and apply them in particular to the systems (Model I and Model II) at hand, which serve as a guidance for the search for cluster crystals on the basis of the monomer-resolved models.

At sufficiently high densities ρ, where $\rho = N/V$ is given by the number of dendrimers N per volume V, it has been shown that the direct correlation function $c(r)$ is, to an excellent approximation, related to the pair-interaction $\phi(r)$ by[19,28,29,45]

$$c(r) = -\beta\phi(r). \tag{3}$$

Eq. (3) is similar to the mean spherical approximation, taking additionally into account that there is no short range excluded volume contribution present. In combination with the Ornstein-Zernike relation,[46] the static structure factor $S(q)$ in the MFA is written as

$$S(q) = \frac{1}{1 + \beta\rho\hat{\phi}(q)}, \tag{4}$$

where q is a wavenumber. Within the MFA, the presence of negative Fourier components in the effective pair-interaction causes an upper density limit to the stability of a homogeneous fluid phase, because for the corresponding wavenumbers q, the structure factor in Eq. (4) would diverge and become negative on increasing ρ at fixed T; the same holds for lowering T at fixed ρ. Therefore, if we denote by q_* the value of the wavenumber q at which $\hat{\phi}(q)$ attains its (negative) absolute minimum, we obtain the so-called λ-line in the density-temperature diagram $k_B T_\lambda = |\hat{\phi}(q_*)|\rho_\lambda$, also known as the Kirkwood instability.[13]

Based on these theoretical considerations, it was postulated that $Q^{\pm}$ systems will freeze at all temperatures for sufficiently high densities.[19] However, since these particular systems have bounded interactions, the crystals do not necessarily have to form by placing one particle per lattice site as is the case for systems interacting via hard or diverging potentials. Instead, crystals with multiple occupancy can form, i.e., two or more particles forming a cluster can be localized on the same crystal lattice position. With the aid of density functional theory, Likos *et al.*[29] demonstrated that the freezing densities $\rho_\times$ for these type of pair-interactions also lie on a straight line in the density-temperature plane, namely,

$$\rho_\times = \frac{k_B T}{1.393\,|\hat{\phi}(q_*)|}, \tag{5}$$

which preempts the aforementioned Kirkwood instability of the homogeneous fluid ($\rho_\times < \rho_\lambda$ at fixed T). The crystallization line depends on the model only via the value of $\hat{\phi}(q_*)$. Moreover, the average number of particles per lattice site, i.e., average cluster size $N_{\rm occ}$, is found to be proportional to the density,

$$N_{\rm occ} = \frac{\zeta^3}{z q_*^3}\rho, \tag{6}$$

so that the lattice spacing a is independent of ρ,

$$a = \frac{\zeta}{q_*}. \tag{7}$$

The last two quantities depend on the model only through the wavenumber q_* at which the Fourier transform of the pair-interaction attains its minimum value. The constants ζ and z that appear in these expressions are geometrical values corresponding to a specific crystalline structure under

Reuse of AIP Publishing content is subject to the terms: https://publishing.aip.org/authors/rights-and-permissions. Downloaded to IP: 91.115.166.109 On: Mon, 23 May 2016 16:29:26

consideration. In particular, one finds $(\zeta, z) = (2\sqrt{2}\pi, 2)$ and $(2\sqrt{3}\pi, 4)$ for the BCC and FCC crystal, respectively.[29]

Despite their approximate character, stemming from both the zero-density effective potential approximation and the MFA on the same, the above results serve as a first estimate of the region of interest in which stable cluster crystals of the real systems could be found; one needs, therefore, to relate the numbers of the MFA-predictions to the microscopic parameters of the specific models at hand. To this end, we list in Table II the most important quantities for both models and the corresponding predictions for the freezing transition.[43] The wavevector q_* where the Fourier transform of the effective pair-potential attains its minimum value, $\hat{\phi}(q_*)$, is obtained from simulation results as shown in Fig. 2. The predicted value for the freezing-density, $\rho_\times$, pertains to the BCC-crystal[29] but the corresponding one for the FCC-crystal is close. Numerically, the values $\rho_\times\sigma^3$ are rather low, but one needs to keep in mind that these are the dendrimer densities reduced over the volume σ^3 of the core monomers. In terms of a volume fraction by means of the size of an isolated dendrimer, R_g^3, these values become $(4\pi/3)\rho_\times R_g^3 = 3.29$ and 0.55 for Model I and Model II, respectively. These densities can alternatively be expressed in the form of a total monomer volume fraction $\eta_\times$, which we define as

$$\eta = \rho\frac{\pi}{6}\left(6\sigma_{\mathrm{CC}}^3 + 8\sigma_{\mathrm{SS}}^3\right), \tag{8}$$

where we have used the values σ_{CC} and σ_{SS} as a measure for the effective diameters of core and shell monomers, respectively. This reveals that freezing is predicted for both models to occur for systems that are moderately dense at the monomer level and dense on the dendrimer level.

Both the average cluster size at the MFA-freezing density, $N_{\mathrm{occ},\times}$, and the corresponding lattice distance a do depend on the crystalline structure at hand via the geometric constants ζ and z. For this reason, these properties are only listed for the BCC and FCC crystals, which according to MFA results are expected to be the most relevant structures in these particular systems. The predicted density $\rho_\times$ at which the freezing transition occurs in the case of Model II is more than a factor six lower than for Model I. Of particular importance is the prediction that the average number of dendrimers per cluster required to stabilize the crystal is reduced by more than a factor three in Model II. It is hence to be expected that although qualitatively Models I and II are similar, the second has the advantage of being more easily accessible by simulations, due to its smaller cluster sizes.

TABLE II. The radius of gyration R_g and the wave vector q_* at which the pair interaction is minimal for both dendrimer models. The predicted values for the freezing transition are labeled by ×. The average cluster size at freezing $N_{\mathrm{occ},\times}$ and the corresponding lattice distance a are only given for the BCC and FCC crystal structures.[43]

	Model I		Model II	
R_g/σ	3.37		3.58	
$q_*\sigma$	0.95		0.74	
$\beta\hat{\phi}_{\mathrm{eff}}(q_*)/\sigma^3$	−35		−249	
$\rho_\lambda R_g^3$	1.094		0.185	
$\rho_\times\sigma^3$	0.021		0.0029	
$\rho_\times R_g^3$	0.785		0.133	
$\eta_\times$	0.358		0.198	
	BCC	FCC	BCC	FCC
$N_{\mathrm{occ},\times}$	8.5	7.8	2.5	2.3
a/σ	9.4	11.5	12.0	14.7

IV. THE LIQUID PHASE

To investigate systems at finite concentrations, we employ Monte Carlo simulations in the canonical ensemble, in which a constant number of N dendrimers are simulated at a fixed volume V and fixed temperature T. In the case of the liquid phase, $N = 250$ dendrimers are simulated in a cubic simulation box with periodic boundary conditions.[47] The Monte Carlo moves consist of individual monomer translations as well as random translational and rotational moves of whole dendrimers. The initial configurations are obtained by slow, incremental compression of equilibrated systems at lower densities. Since the liquid phase for Model I has already been discussed in detail in Ref. 7, we will concentrate here on the results for Model II at three representative densities.

The system with the lowest density, $\rho R_g^3 = 0.046$, corresponds to a gas or low density fluid. The intermediate system has a density $\rho R_g^3 = 0.138$, which slightly exceeds the MFA-predicted freezing density $\rho_\times R_g^3 = 0.133$. The highest density, $\rho R_g^3 = 0.323$, that we consider for the above liquid-like behavior, lies about 35% above the overlap concentration and is well beyond even the upper limit of stability of the homogeneous fluid, $\rho_\lambda R_g^3 = 0.185$, predicted on the basis of the effective dendrimer pair-interaction. In fact, it turns out that this lies above the crystallization density found by MC simulations of the microscopic model, see Section V. Accordingly, at this density we are looking into a metastable fluid, owing its existence to the particular preparation of the system.

In order to characterize the fluid phase, we consider the radial distribution function $g(r)$ of the centers of mass of the dendrimers as shown in Fig. 3. The striking emergence

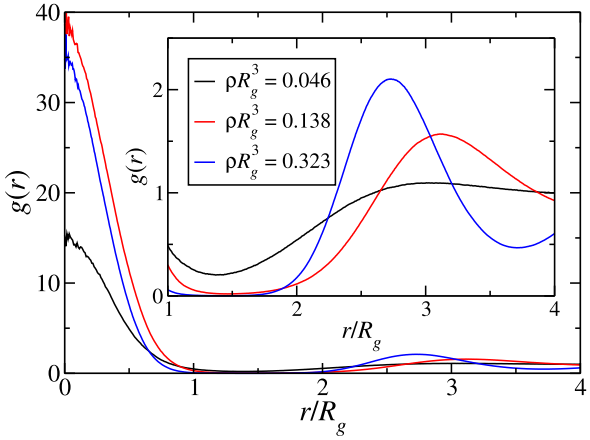

FIG. 3. The radial distribution function $g(r)$ for the centers of mass of the dendrimers of Model II for three different densities, as indicated in the panel.

Reuse of AIP Publishing content is subject to the terms: https://publishing.aip.org/authors/rights-and-permissions. Downloaded to IP: 91.115.166.109 On: Mon, 23 May 2016 16:29:26

of a broad peak located at zero-distance upon increasing the density is a feature that signifies the existence of clusters in these systems and implies that the centers of mass of the dendrimers can get arbitrarily close to one another. At large separations, one finds the typical oscillatory behavior known from conventional fluids, for which upon increasing the density the fluid gets locally more structured. The fact that the height of the central peak increases non-monotonically with density has no particular significance, as it is only after multiplication with the density and performing the corresponding 3D integration up to the first minimum that the peak corresponds to the average number of dendrimers per cluster.

The number of particles per cluster has been calculated counted by employing the algorithm that was described in detail in Ref. 7, which allows one to separate clusters that share a common particle. The resulting probability distributions $P(N_{\mathrm{occ}})$ of the cluster occupation numbers N_{occ} and the probability $P(\mathrm{D} \in N_{\mathrm{occ}})$ for a dendrimer to be found in a cluster of size N_{occ} are, together with representative snapshots of the simulations, shown in Fig. 4 for the three densities considered. Combining the information from Figs. 3 and 4, we find that the system with the lowest density indeed behaves as a low-density gas. On average, the dendrimers avoid one another due to the repulsion of the shell monomers, but they do approach each other occasionally to form rare clusters of up to five dendrimers. The relative probabilities of these clusters indicate that the short-range attraction found in the effective pair-interaction does play an important role in their stabilization. In fact, even at this low density where about 90% of the dendrimers remain isolated, the most likely multi-particle cluster for a dendrimer to be found in is of size four. The clusters themselves are not well-defined in shape and there is still a vivid in- and out-flux of particles, which is also reflected by the shallow and broad minimum of the $g(r)$ between the central and first neighbor peak taking a finite value of about 0.2.

Upon increasing the density to $\rho R_g^3 = 0.138$, the cluster size probability distribution changes significantly. The most prominent size is still the single dendrimer cluster, but it contains only about 15% of all the particles, whereas 50% of all dendrimers is found to be in a cluster of size four. The first minimum of $g(r)$ drops to a value of 0.02, which implies more well-defined clusters, as can also be seen from the corresponding snapshot. An increased density also results into enhanced stabilization of the formed clusters, allowing them to grow up to six dendrimers and resulting in a more pronounced first-neighbor peak in the $g(r)$ at a distance $r \cong 3R_g$.

At the highest density, $\rho R_g^3 = 0.323$, where, according to the MFA-prediction, the system should already have crystallized, almost no single dendrimers exist. The cluster size distribution shifts to larger values and results in an average cluster size of 4.7 dendrimers. As can be readily seen in the snapshot, the clusters themselves are now easily identifiable, and the first neighbor peak in the radial distribution function is shifted to $r \cong 2.8R_g$. In the range $R_g \lesssim r \lesssim 2R_g$ a depletion zone arises, in which $g(r) \leq 0.01$, separating dendrimers within the same cluster from those belonging to a neighboring cluster. The fact that the radial distribution functions does not vanish completely implies that an exchange of individual dendrimers between clusters does take place.

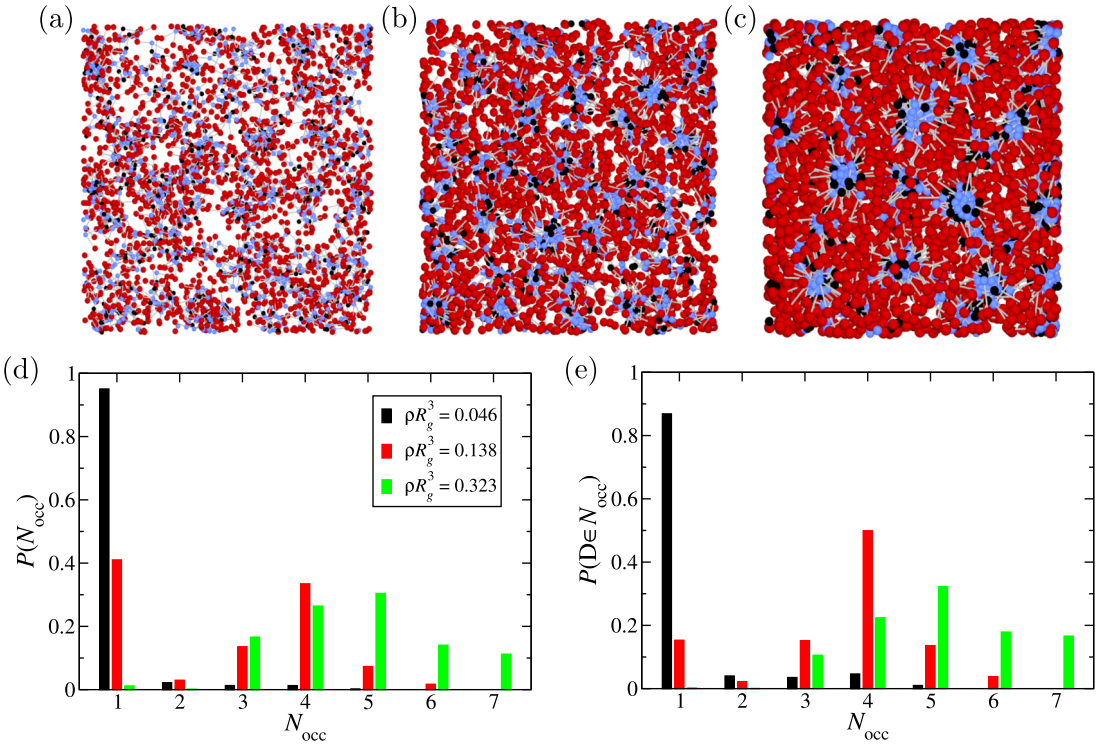

FIG. 4. Typical snapshots from the simulations of Model II systems at densities (a) $\rho R_g^3 = 0.046$, (b) $\rho R_g^3 = 0.138$, and (c) $\rho R_g^3 = 0.323$, where the generation 0, 1, and 2 monomers (not drawn to scale) are shown in black, blue, and red, respectively. (d) presents the probability $P(N_{\mathrm{occ}})$ of a cluster being formed by N_{occ} dendrimers. (e) shows the probability $P(\mathrm{D} \in N_{\mathrm{occ}})$ for a dendrimer to be found in a cluster of size N_{occ}.

Reuse of AIP Publishing content is subject to the terms: https://publishing.aip.org/authors/rights-and-permissions. Downloaded to IP: 91.115.166.109 On: Mon, 23 May 2016 16:29:26

No spontaneous crystallization was found in the system, despite the fact that visual inspection [e.g., of Fig. 4(c)] gives the impression of local, BCC-type ordering. This is not surprising, since it is known also from simpler systems that the compatibility between box size/shape and lattice constant, as well as other finite size effects can hinder the spontaneous formation of periodic crystals in a simulation. In our case, these difficulties are exacerbated by the fact that the crystals have multiple and variable occupancy and that the dendrimers would have to diffuse and self-organize on the cluster sites, making thus the process computationally very expensive. Still, the broad depletion region between neighboring clusters found at the highest density is an indication of an incipient order in which the clusters are well-separated from one another, as it happens for periodic crystals. In the absence of spontaneous crystallization, different computational strategies to investigate the formation of cluster crystals have to be employed. These are presented in Sec. V.

V. CLUSTER CRYSTALS

The formation of cluster crystals in the effective pair-potential picture of the $Q^{\pm}$-class is a well-established fact.[18,20] Given the indications of the cluster fluid seen in Sec. IV, it is only natural to ask whether the models of amphiphilic dendrimers at hand can form stable cluster crystals. As a first step to answering this question, we artificially construct such crystals *by hand* and analyze their stability. Although it is not *a priori* clear which crystalline structure would be stable, we will limit ourselves to considering the BCC and FCC crystals only, on the one hand because they are the most common structures and on the other because they are the ones occurring within the effective-potential picture.[18,20] A second simplification we make is to consider perfect cluster solids, i.e., we place on every lattice site of the crystal monodisperse clusters, all sharing the same occupation number N_{occ}. The crystals are constructed by placing the centers of mass of exactly N_{occ} dendrimers with randomized conformations on each of the lattice positions. For computational reasons we restrict ourselves to mainly $2^3 = 8$ unit cells with periodic boundary conditions, but some of the results have been verified for a larger system size of $3^3 = 27$ unit cells.

Each of the crystals that have been considered can be identified by its structure, BCC or FCC, and a combination of density and occupation number (ρ, N_{occ}). For ordinary crystals, the density would have been sufficient, but for cluster crystals there are different combinations of cluster occupancy and lattice distance corresponding to the same density. Of course, at thermodynamic equilibrium there is no additional degree of freedom, since N_{occ} is selected as the value that minimizes the free energy; however, this value is not known *a priori*. In an initial equilibration phase, the centers of mass are constrained by an external potential, while the internal structure of all dendrimers is allowed to equilibrate. Thereafter, the constraints on the centers of mass are slowly released and the simulations are continued in the unconstrained canonical ensemble. Two examples of crystals that are mechanically stable are shown in Fig. 5, in both a monomer-resolved representation and a coarse-grained fashion by using the centers of mass of the dendrimers only; the latter enables one to identify the clusters more easily. The larger spheres indicate the range in which the centers of the dendrimers are found, and they therefore represent

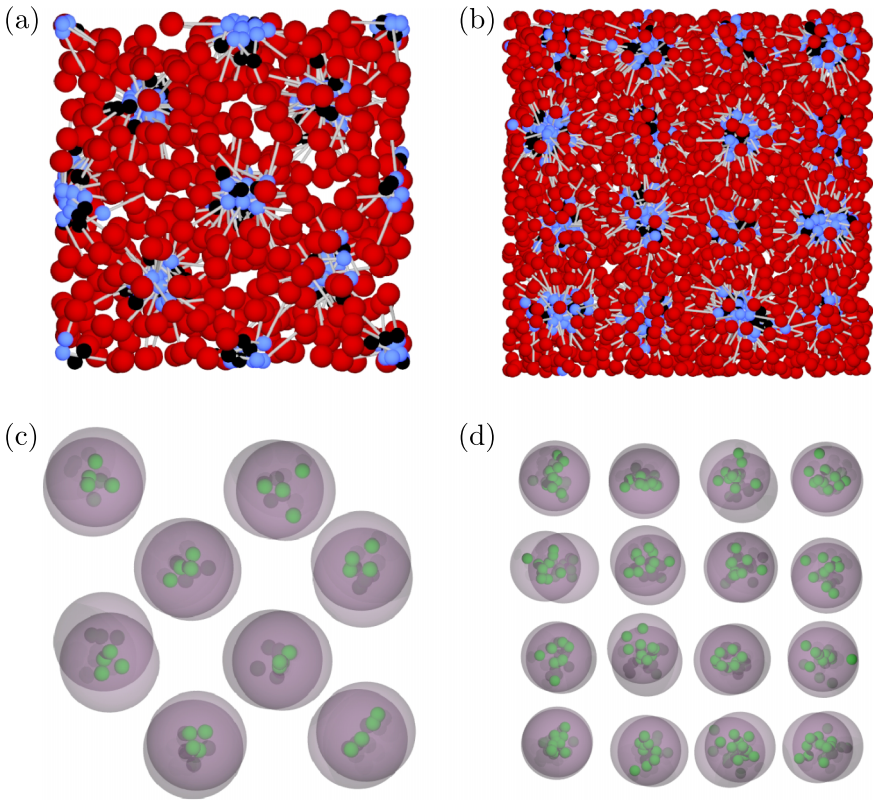

FIG. 5. Simulation snapshots of mechanically stable cluster crystals of Model II. Panel (a) shows a BCC crystal with $N_{\mathrm{occ}} = 4$, $\rho R_g^3 = 0.281$ and (b) a FCC crystal with $N_{\mathrm{occ}} = 10$, $\rho R_g^3 = 0.480$. For clarity, monomers are not drawn to scale. Panels (c) and (d) depict the same systems, but only show the centers of mass of the dendrimers (green) and the size of clusters.

Reuse of AIP Publishing content is subject to the terms: https://publishing.aip.org/authors/rights-and-permissions. Downloaded to IP: 91.115.166.109 On: Mon, 23 May 2016 16:29:26

the localization and confinement of dendrimers within their cluster.

For both density and cluster occupation, there exist lower limits below which the dendrimer crystals are found to be mechanically unstable. In the former case, the cluster positions start diffusing, whereas for the latter case the clusters cannot withstand the external pressure by other clusters, which are too close to them, and start to merge. These processes are relatively fast in destabilizing the initial perfect ordering. There is, however, a wide range of parameters for which the cluster crystals remain mechanically stable, even for simulations times orders of magnitude longer than for the unstable ones. This gives rise to a mechanically stable cluster crystal region as is shown in Fig. 6 for Model I in the case of FCC crystals.

Although based on a limited set of data points, the minimum density that is required to stabilize a cluster crystal is estimated to be $\rho R_g^3 \cong 1.0$. This value lies below that of the Kirkwood instability at $\rho_\lambda R_g^3 = 1.094$ but is significantly higher than the predicted freezing density $\rho_\times R_g^3 = 0.785$ that was estimated based on the effective pair-interaction for Model I (see Table II). The MFA-prediction for the cluster occupancy, $N_{\rm occ} \cong 8$ at freezing, is very close to the minimum occupancy required for mechanic stability. This proximity of the two values already shows that a theory based on effective pair-interactions can serve as a guideline to estimate the relevant range of parameters. At the same time, however, it should be kept in mind that mechanical stability is a necessary but not sufficient requirement to guarantee thermodynamic stability.

The requirement of more than 8 dendrimers per cluster to stabilize a cluster crystal is very CPU-demanding; this is the main reason for having introduced Model II in Ref. 39, which predicts clustering at lower densities and occupancies, and thus enables us to perform a more detailed analysis of the phase behavior. The main results for the mechanical stability of the BCC and FCC cluster crystals in this particular model are shown in Fig. 7. The results are similar to those of Model I and, again, at the predicted freezing density $\rho_\times R_g^3 = 0.133$ (vertical dotted lines in Figs. 6 and 7) the crystals are unstable. Contrary to the case of Model I, even

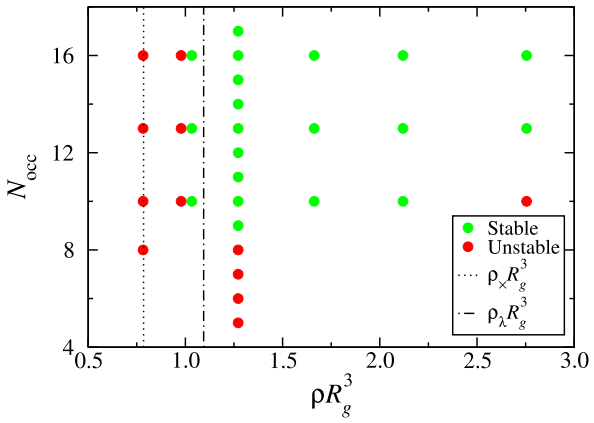

FIG. 6. The cluster size $N_{\rm occ}$ versus density ρR_g^3 phase diagram of mechanical stability for FCC crystals of Model I. Stable systems are marked in green, unstable systems in red. The dotted and dashed-dotted lines are the densities for the predicted freezing and the Kirkwood instability, respectively.

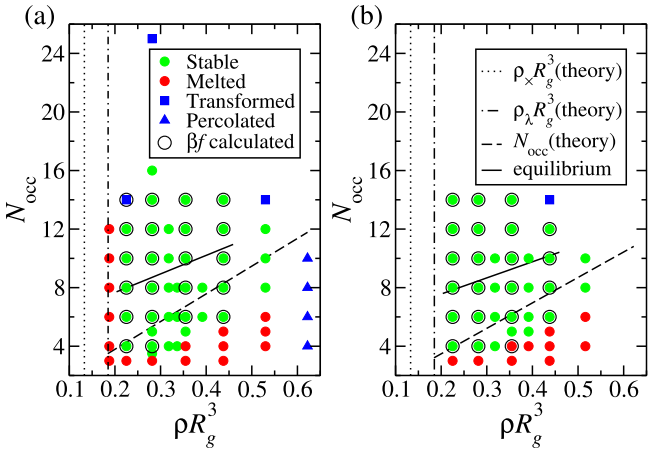

FIG. 7. Mechanical stability diagrams for (a) BCC and (b) FCC crystals for Model II. Stable systems are marked in green, unstable in red or blue. Systems for which the free energy was computed are marked with a black circle. The dotted, dotted-dashed, and dashed lines represent the theoretically predicted freezing densities, Kirkwood instability, and cluster occupancies, respectively. The solid lines are the actual stable occupancies as function of the density for either crystal types.

at the MFA-Kirkwood instability (dashed-dotted lines), the crystals are not mechanically stable. In addition, the predicted minimum cluster occupancy is underestimated, because no crystal with fewer than four dendrimers per cluster could be stabilized.

Even more intriguing is the fact that the region of stable crystals is bounded from above in both cluster occupation and density, which is absent in the case of the effective pair-interaction description.[2,17,19] The two upper limits are described by two different scenarios and their existence is a direct consequence of the breakdown of the pair-interaction approximation. For a few selected densities, the cluster occupancy was probed at higher values, at the cost of larger lattice distances. In such cases, the crystals became deformed while keeping the cluster size intact, suggesting a preference to form different crystalline structures from the one originally imposed or a transition to different occupancy which was hindered by finite box-size effects. Increasing the density while keeping the cluster occupancy fixed, in other words reducing the lattice spacing, resulted in a situation where the clusters start to percolate. The three different types of instability we found — melting, transforming, and percolating — are indicated by different colors in Fig. 7. Whether deformation or percolation would be the final outcome or just are precursors of a different phase is yet unknown. Irrespectively, this finding signifies that cluster crystals built of Model II-dendrimers can only be mechanically stable in a limited region of the density-occupancy space.

VI. STRUCTURAL ANALYSIS

We have seen in Sec. V that a description of cluster crystals based on the validity of the effective pair-interaction from the infinite dilution limit fails to yield correct results for higher densities. The reason must lie in the fact that the dendrimers undergo substantial deformations as density

Reuse of AIP Publishing content is subject to the terms: https://publishing.aip.org/authors/rights-and-permissions. Downloaded to IP: 91.115.166.109 On: Mon, 23 May 2016 16:29:26

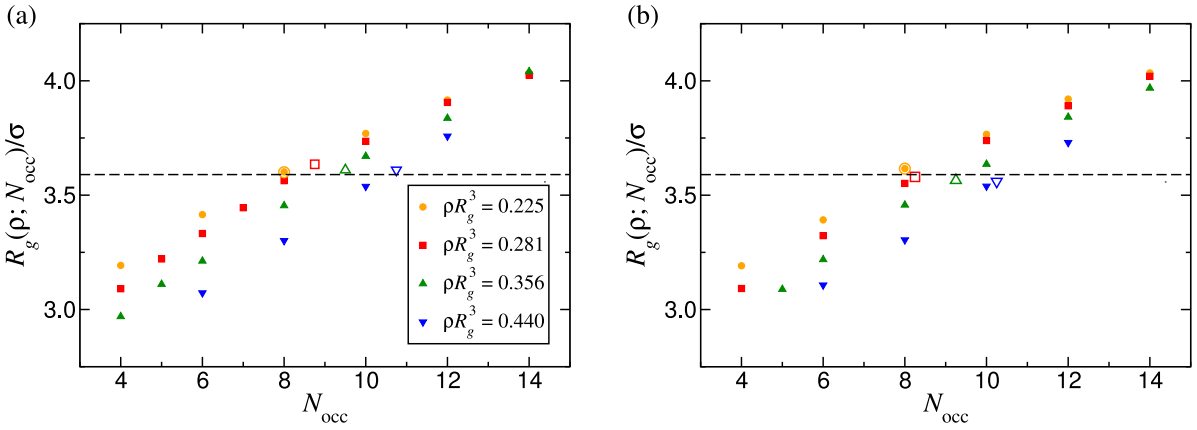

FIG. 8. The radius of gyration $R_g(\rho; N_{occ})$ of Model II dendrimers in (a) BCC and (b) FCC crystals. The open symbols denote the value for the thermodynamically stable crystals at the corresponding densities. The horizontal line indicates the value $R_g = 3.58\sigma$ of the gyration radius of the dendrimers at infinite dilution.

grows, so that the infinite-dilution effective interaction loses its validity. To investigate this further, we focus here on the analysis of the internal structure of individual dendrimers and its dependence on the density. To this end, we measured a number of structural characteristics for Model II within the various mechanically stable BCC and FCC clusters, as indicated in Fig. 7. The first quantity is the radius of gyration; results are shown in Fig. 8 and reveal that in either crystal types the radius of gyration $R_g(\rho; N_{occ})$ at fixed density ρ grows almost linearly with the cluster occupancy N_{occ}. In addition, it diminishes on increasing the density at constant N_{occ}. Both trends can be understood from the cluster crystal structure. Fixing the density and increasing the number of dendrimers per cluster brings about an increase of the lattice spacing between the cluster-occupied crystal sites. This leads to a decrease of the forces on a cluster exerted by the neighboring ones and thus the dendrimers in the cluster swell. Increasing ρ at fixed N_{occ} causes the lattice constant to diminish and the opposite effect, i.e., a shrinking of the dendrimers, results. It should be stressed that these trends are not equilibrium properties of the system. As will be demonstrated by means of a free energy calculation in Sec. VII, there exists an optimal cluster size as function of the density for each crystal — the one that minimizes the crystal's free energy among all cluster sizes at given ρ. In Fig. 8 the equilibrium results for each of the densities are indicated by open symbols. Surprisingly, these equilibrium values almost coincide with the value $R_g = 3.58\sigma$ of an isolated dendrimer.

The radius of gyration R_g is only a very rough measure of the structure of the molecule, merely expressing its overall size. More detailed information can be obtained by the monomer profiles of each dendrimer. In Fig. 9, we show single-dendrimer density profiles $c(r)$ of the core and shell monomers with respect to the center of mass of a dendrimer in a cluster crystal. Results pertain to a FCC cluster crystal at density $\rho R_g^3 = 0.281$ for different cluster occupancies in Fig. 9(a) and to fixed cluster size $N_{occ} = 8$ and various densities in Fig. 9(b), where it should be noted that the combination $\rho R_g^3 = 0.281$ and $N_{occ} = 8$ is very close to the thermodynamic equilibrium. The profiles measured for the BCC crystal are not shown, but they coincide almost perfectly with the FCC profiles for matching density and cluster size.

The increase in radius of gyration seen in Fig. 8, on either increasing the cluster size at fixed density or on lowering the density at fixed cluster size, can also be observed in Fig. 9 of single dendrimer density profiles $c(r)$ by the decrease in the $r = 0$ maximum of the core distributions, and a broadening and shifting to larger distances for the shell distributions.

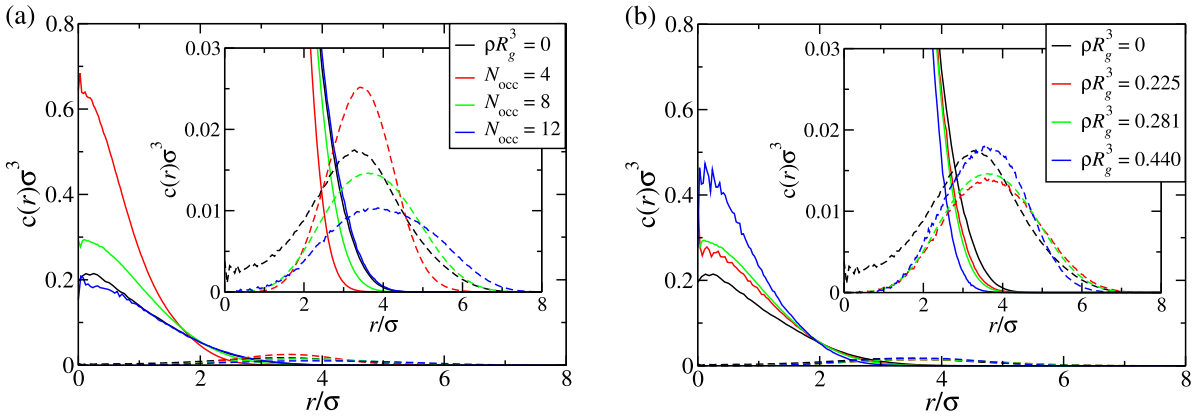

FIG. 9. Single-dendrimer monomer-density profiles $\rho(r)$ with respect to the Model II-dendrimer center of mass in FCC cluster crystals for (a) fixed density $\rho R_g^3 = 0.281$ and (b) fixed cluster size $N_{occ} = 8$. Solid lines correspond to the core monomers, dashed curves to the shell monomers. Insets are enlargements focusing on the shell monomer profiles. For comparison, the density profiles as found for an isolated dendrimer are shown in black.

Reuse of AIP Publishing content is subject to the terms: https://publishing.aip.org/authors/rights-and-permissions. Downloaded to IP: 91.115.166.109 On: Mon, 23 May 2016 16:29:26

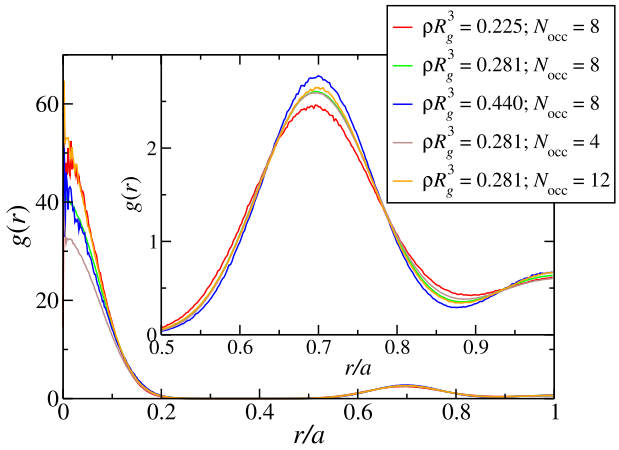

FIG. 10. Radial distribution function $g(r)$ for the center of mass of Model II dendrimers in various FCC crystals, where the distance r is given in terms of the lattice constant a.

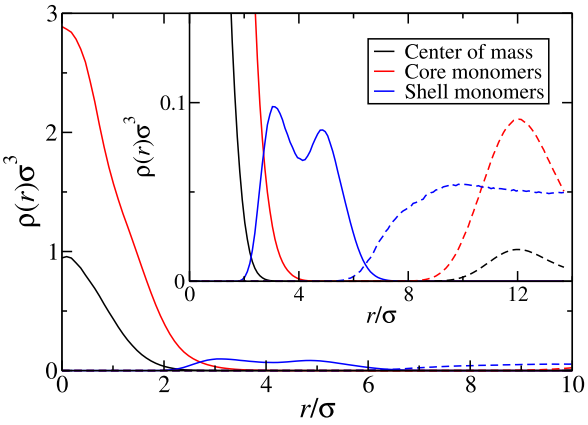

FIG. 11. Density profiles of the centers of mass, core, and shell monomers of Model II-dendrimers with respect to the center of mass of the cluster for a BCC crystal with $\rho R_g^3 = 0.281$ and $N_{occ} = 8$. The solid curves represent contributions stemming from the same cluster, whereas the dashed curves in the inset are contributions from dendrimers belonging to different clusters.

The profiles for an isolated dendrimer are indicated as well, and they demonstrate that although the radius of gyration in equilibrium is almost constant, the actual internal structure of the dendrimer is different and depends on both the overall density and cluster occupation number. In particular, the back-folding of shell monomers into the core observed for an isolated dendrimer is strongly suppressed in the cluster crystals. The core and shell monomers have an enhanced propensity to segregate in the cluster crystals, thus forming a somewhat more compact and denser core as well as a more distant and lower density shell compared to the isolated molecule. This behavior arises from the interactions between dendrimers within the same and from surrounding clusters. The two tendencies of the core (more compact) and the shell (more spread) monomers are antagonistic to one another as far as their effect on the gyration radius of the whole molecule is concerned. Accordingly, they bring about the finding that in equilibrium cluster crystals the radius of gyration remains nearly unaffected with respect to its value at infinite dilution despite the fact that the dendrimers' conformations are affected by the finite concentration in very significant ways.

The correlation between the centers of mass of the dendrimers is measured by means of the radial distribution function $g(r)$. This quantity, for various FCC crystals, is shown in Fig. 10. By plotting the distance in units of the lattice constants, the curves essentially superimpose, with only minor changes due to the different average number of dendrimers per cluster N_{occ} at short ranges, and slightly more compact clusters at higher densities. The latter can be seen from the peak at $r = a/\sqrt{2}$, corresponding to dendrimers in the nearest-neighbor clusters. The relatively broad depletion zone in the range 0.2–0.5a allows us to easily identify the cluster dendrimers belong to. At the same time, it facilitates the determination of whether a specific density and cluster size combination is mechanically stable or not.

The radius of gyration, density profiles, and correlation functions discussed above and shown in Figs. 8-10 are all properties where the individual dendrimers are the focus of attention. The stability of cluster crystals, however, crucially relies on the interplay between the dendrimers within the entities that form the crystal. To this end, we will for the remainder of this section examine the collective behavior of dendrimers by analyzing the structure of the clusters. Fig. 11 shows the density profiles $\rho(r)$ of the center of mass of dendrimers, the core, and the shell monomers with respect to the center of mass of the cluster for a BCC crystal at density $\rho R_g^3 = 0.281$ and cluster size $N_{occ} = 8$. In agreement

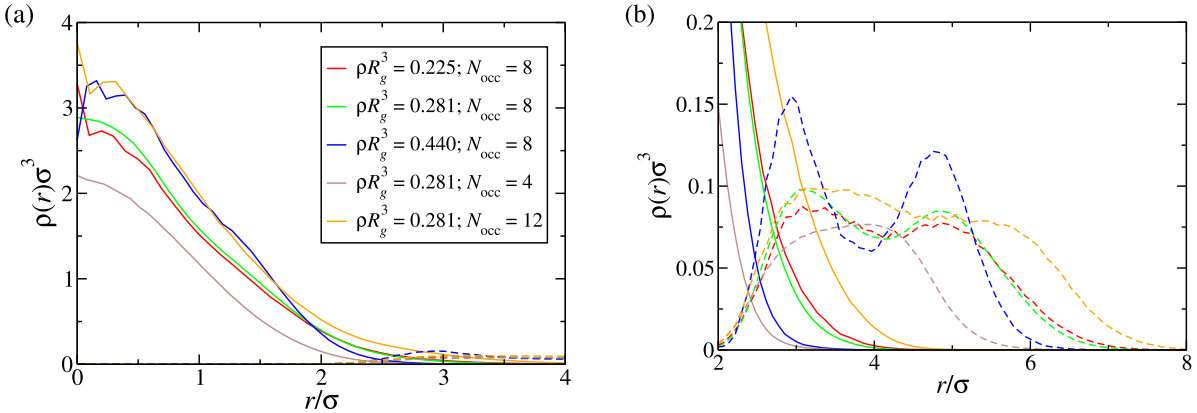

FIG. 12. Radial density profiles for all core and shell monomers with respect to the center of a mass of the cluster in BCC crystals for various combinations of average cluster size and density. The solid curves and dashed curves correspond to profiles of core and shell monomers, respectively.

Reuse of AIP Publishing content is subject to the terms: https://publishing.aip.org/authors/rights-and-permissions. Downloaded to IP: 91.115.166.109 On: Mon, 23 May 2016 16:29:26

with the findings illustrated in Fig. 10, which show a clear separation between the clusters, we find here that also the core and shell monomers belonging to different clusters remain well separated; only a very small fraction of shell monomers from the nearest-neighbor clusters overlaps. Furthermore, the two species of monomers within the same cluster hardly mix, forming a dense core cluster, where the core consists mainly of core monomers, surrounded by a lower density cloud of shell monomers. Although the shell is formed only by the second generation monomers, it nevertheless shows a double peaked structure. This is another illustration of the fact that the internal structure of these particles within the dense cluster crystal is very different from the one at infinite dilution.

A few additional, selected density profiles of core and shell monomers measured with respect to the center of mass of the cluster in BCC crystals are shown in Fig. 12. Both an increase of the density at fixed occupation number and a decrease of the occupation number at constant density, result in a shrinking of the inter-cluster separation. Concomitantly, a more compressed distribution of cores is obtained under these changes. The profiles of the cluster shell, however, are affected more and we can find either single or double layered structures. The latter are formed mainly at the higher densities and suggest the increasing importance of the steric interactions between shell monomers within a cluster. The crowding of these repulsive monomers is probably responsible for mechanically instability of the cluster crystals at high densities, indicated in Fig. 7.

VII. THERMODYNAMIC STABILITY

The preceding findings, summarized in Figs. 6 and 7, establish that in the density-occupation plane, a region of mechanically stable cluster crystals exists. Mechanical stability is a necessary but not sufficient condition for thermodynamic stability. The unstable crystals that melt, deform, or start to percolate within relatively short simulation times are, evidently, thermodynamically unstable. However, for those crystals that remain stable within the simulations, free energy calculations are required to determine which one possesses the lowest free energy among all competing candidate phases.

To compute the Helmholtz free energy, the technique of thermodynamic integration can be employed.[47,48] This method relates the free energy of the system at hand with a suitably chosen reference system of known free energy. With $\Phi(\{\vec{r}\})$ denoting the interaction of the system under study in terms of the set of all particle coordinates, $\{\vec{r}\}$, and $\Phi_{\text{ref}}(\{\vec{r}\})$ its counterpart for the reference system, thermodynamic integration requires a smooth interpolation connecting the two. The simplest choice is given by a linear interpolation via a dimensionless parameter λ

$$\Phi_\lambda(\{\vec{r}\}) = \lambda\Phi(\{\vec{r}\}) + (1-\lambda)\Phi_{\text{ref}}(\{\vec{r}\}), \tag{9}$$

which for $\lambda = 0$ and $\lambda = 1$ corresponds to the reference system and to the system of interest, respectively. Using this family of systems, the Helmholtz free energy $\mathcal{F}$ can be obtained from

$$\mathcal{F} = \mathcal{F}_{\text{ref}} + \int_0^1 d\lambda \langle \Phi - \Phi_{\text{ref}} \rangle_\lambda, \tag{10}$$

where $\mathcal{F}_{\text{ref}}$ is the free energy of the reference system and $\langle \ldots \rangle_\lambda$ denotes an ensemble average for a system interacting via $\Phi_\lambda(\{\vec{r}\})$. Since for determining the thermodynamic stability of the various crystal structures, only their difference in free energy is required; the actual free energy of the reference system does not have to be evaluated, provided the same is being used for all candidates.

One crucial restriction on the reference system is that while varying the parameter λ the system should not exhibit a first-order phase transition. We therefore have to ensure that the reference system is thermodynamically stable in the target crystalline structure. An oft-employed reference system for the computation of free energy of crystals is the Einstein solid, in which each particle is bound by a harmonic potential to a unique lattice site.[47] Such an approach allows to formally separate the total interaction of the reference system in two contributions

$$\Phi_{\text{ref}} = \Phi_{\text{int}} + \Phi_{\text{lattice}}, \tag{11}$$

which are the internal interaction between the particles and the external potential coupling the particles to the underlying crystal structure.

For the present systems that exhibit cluster crystals, the particular choice of an Einstein crystal would not be suitable, due to the intrinsically different nature of a cluster crystal. Contrary to usual solids, here multiple particles can be assigned to a single lattice site and, in addition, they are able to hop to neighboring lattice positions.[23] Therefore, we employ a modified version of the method introduced by Mladek *et al.*,[49] which is based on an ideal gas with confinement cells compatible with the crystalline structure under consideration.

A confining potential is acting on the center of mass $\vec{r}_i^{\,(\text{cm})}$ of each dendrimer i. If we now denote by $\vec{R}_j$ a lattice position of the underlying, perfect crystal structure we choose to consider, the interaction between the dendrimers and the lattice positions can be written as

$$\Phi_{\text{lattice}} = \sum_{i=1}^{N} \Phi_{\text{conf}}\left(\min_j \left| \vec{r}_i^{\,(\text{cm})} - \vec{R}_j \right| \right), \tag{12}$$

where $\Phi_{\text{conf}}(r)$ is the interaction strength between the center of mass of a dendrimer and the lattice position. Its functional form is not unique, but a particularly simple and convenient choice is given by a step function

$$\Phi_{\text{conf}}(r) = \begin{cases} 0 & r \le R_{\text{cut}} \\ U_{\max} & r > R_{\text{cut}} \end{cases}, \tag{13}$$

with R_{cut} a suitably chosen width of the potential well as is schematically shown in Fig. 13 for an one-dimensional analog. The "free volumes" $v_0 = (4\pi/3)R_{\text{cut}}^3$ around each crystal site are not allowed to overlap and they must be small enough to keep the crystals from melting. In order to make a reference system that resembles the structure of the dendrimer crystals as much as possible, we choose $R_{\text{cut}} = 2\sigma$, which is the typical width of the distribution of centers of mass of the dendrimers in a cluster, as measured in the simulations that showed mechanical stability (Fig. 7). The height of the energy penalty

Reuse of AIP Publishing content is subject to the terms: https://publishing.aip.org/authors/rights-and-permissions. Downloaded to IP: 91.115.166.109 On: Mon, 23 May 2016 16:29:26

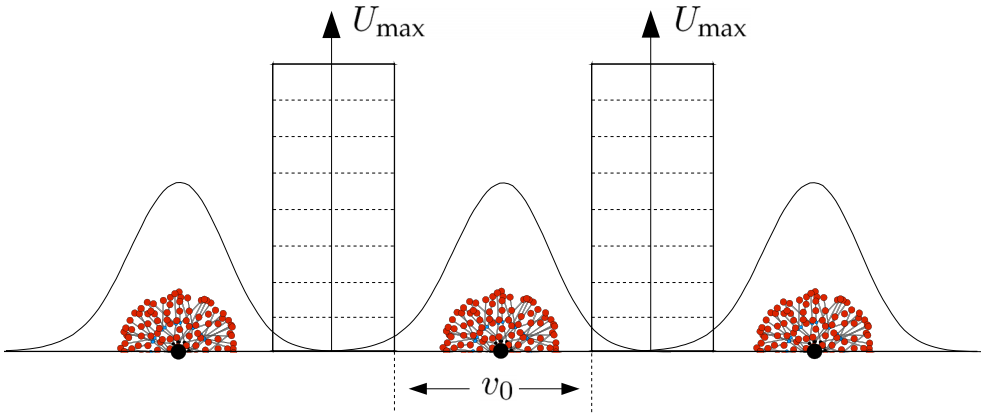

FIG. 13. One-dimensional, schematic representation of the confining potential used in the free energy calculations for cluster crystals. The solid curves represent the density distributions around the lattice sites (black circles). The quantity $U_{\max}$ is the barrier height, see Eq. (13), whereas v_0 indicates the volume left between neighboring barriers in which the particle is free of external influences.

was fixed to a value $U_{\max} = 10\,k_{\mathrm{B}}T$. This finite value allows for dendrimers to explore the full volume of the simulation box and hop to clusters located at neighboring lattice positions and is necessary to hold the multi-occupancy crystal together and relax its site occupation.

The process of hopping requires a dendrimer to be removed from one and inserted within another cluster. The inter-monomer interactions by means of the Morse potential make this a rare event. In order to facilitate such hopping events, we can make use of the freedom provided by the choice of the internal interaction Φ_{int}, restricting it to the FENE potentials between bounded monomers of the same dendrimer only, i.e.,

$$\Phi_{\mathrm{int}} = \sum_{(ij)} \Phi^{\mathrm{FENE}}_{\mu_i \nu_j}\left(|\vec{r}_i - \vec{r}_j|\right), \tag{14}$$

where $\vec{r}_i$ and $\vec{r}_j$ are the positions of the monomers i and j, respectively, and μ_i and ν_j the corresponding types labels for a core or shell unit. The summation runs over all pairs (ij) of monomers that are chemically bonded. Consequently, in the reference system there are no intermolecular interactions, and the intramolecular interactions are only there to maintain the connectivity. This allows for a rejection free movement of dendrimers to different clusters.

The choice of Φ_{ref} means that the reference system consists of non-interacting ideal dendrimers confined to form clusters in the vicinity of one of the lattice positions $\vec{R}$. The average number of dendrimers per cluster can be controlled by choosing the number of dendrimers and the number of lattice positions. The free energy of the reference system itself consists of two contributions, which are corresponding to the internal degrees of freedom of the now ideal dendrimer and that of the external confinement of point particles. Since only the Helmholtz free energy per particle needs to be compared for the thermodynamic stability, the internal degrees of freedom will give rise to the same contribution for all systems.[50]

Using the procedure detailed above, free energy calculations were performed for FCC and BCC cluster crystals of Model II dendrimers with integer occupation numbers. Various densities were selected, lying in the range of mechanical stability, and are indicated in Fig. 7 by black circles. The results from this analysis are presented in Fig. 14(a), where for several densities the excess free energy

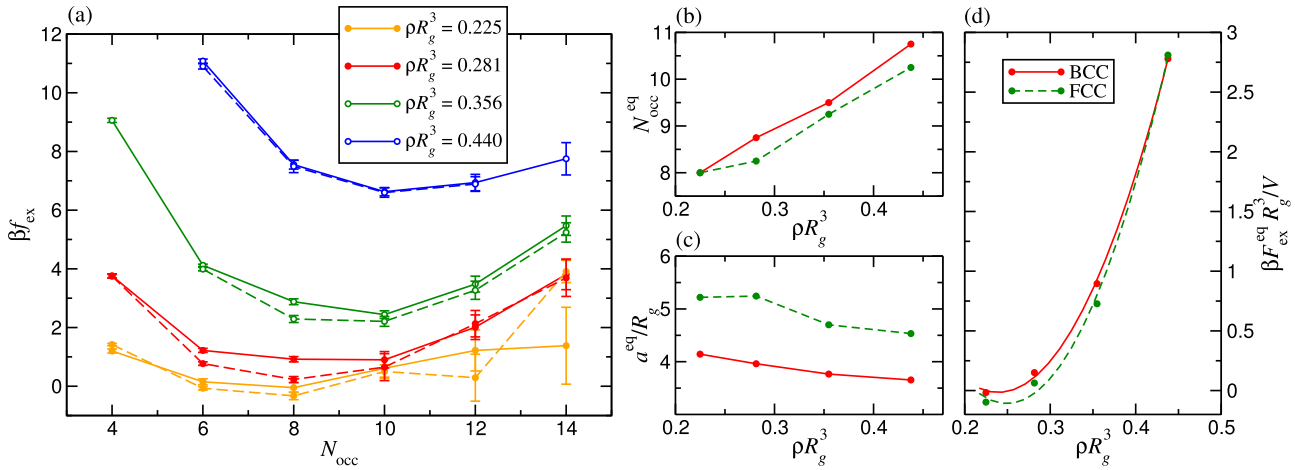

FIG. 14. (a) The excess free energy per particle, βf_{ex}, as a function of the cluster occupancy N_{occ}. The different colors correspond to constant overall densities. The equilibrium properties extracted are the (b) average cluster occupation N_{occ}, (c) lattice constant a, and (d) the excess free energy per volume $\beta F_{\mathrm{ex}}/V$ as function of the overall density ρR_g^3. Solid and dashed lines correspond to BCC and FCC crystals, respectively.

Reuse of AIP Publishing content is subject to the terms: https://publishing.aip.org/authors/rights-and-permissions. Downloaded to IP: 91.115.166.109 On: Mon, 23 May 2016 16:29:26

per particle is shown as function of the cluster occupation number. For each of these densities there is a clear minimum visible, demonstrating that there is an optimal cluster size in the crystals, as dictated by thermodynamics: the quantity N_{occ} is a self-adjusting parameter of the system, which for every density attains the value minimizing the system's (Helmholtz) free energy. From a fit through the data, this optimum value was determined for each of the densities considered. Results in Fig. 14(b) show that the cluster size grows roughly linearly with the density. This is in agreement with the MFA-predictions based on the effective pair interaction but, contrary to these predictions, an extrapolation of the line to vanishing densities shows that the line does not go through the origin.[29] Concomitantly, the equilibrium lattice spacing a^{eq}, shown in Fig. 14(c), decreases on increasing the density, which is at odds with what is expected theoretically,[29] where the lattice constant remains density-independent. This is another indication that the many-particle interactions at play in dense dendrimer solutions lead to deviating behavior from the structure-less particles assumed by an infinite-dilution effective interaction description. However, the effective interaction is remarkably successful not only for *predicting* the occurrence of cluster crystals in the first place but also for making quantitatively correct estimates regarding the range of densities and lattice occupancies for which cluster crystals form and attain thermodynamic stability with respect to the fluid phases at lower densities. As such, and in combination with the fact that the estimates are analytically known, it is of great value for providing reliable guidance for searches within more detailed, microscopic approaches. In the final panel, Fig. 14(d), the excess free energies per particle in equilibrium for both the BCC and the FCC crystal are compared, indicating that the FCC crystal is the more thermodynamically stable one. However, extrapolation of the data hints at a possible preference for BCC crystals at densities even higher than the ones studied here.

In the discussion above, we found that the average cluster occupation in equilibrium by assuming it to be a continuous rather than integer variable. There are two arguments to justify such non-integer occupation numbers. The first is a coexistence of two perfect crystals with different but integer occupation numbers as is, for instance, found at low temperatures in GEM-models.[21,22,51] The second possibility is that, within a crystal, the average occupation number is not fixed, but there is actually a distribution of different cluster sizes present, which are either ordered or randomly positioned within the overall crystalline structure. In order to homogenize the cluster size distribution, clusters have to be formed or dissolved, and dendrimers need to be redistributed over different clusters via the hopping process. Although a detailed analysis concerning this issue has not been performed yet, preliminary results suggest the latter scenario. This assertion is based on the observation that crystals with artificially created defects remained mechanically stable. The defects considered included perfect crystals with an individual cluster containing a different number, either smaller or larger, than the rest of the system, but also the removal of a complete cluster. In all these cases defects appeared not to have any significant effect on the surrounding crystal. Only for the lowest occupation number $N_{\mathrm{occ}} = 4$ the removal of a cluster resulted in a situation where dendrimers from neighboring clusters diffused to the empty space in order to heal the defect.

VIII. CONCLUSIONS

We have demonstrated by means of computer simulations that the formation of soft cluster crystals is not merely a mathematical property of the $Q^{\pm}$-class of model interaction potentials, but it can be found for realistic models of relatively simple macromolecules. In particular, we have shown this to be the case for second generation amphiphilic dendrimers by explicit free energy calculations, using a thermodynamic integration method specifically designed for these type of phases. Upon augmenting the density, the model dendrimers extensively discussed here were found to form a cluster fluid in which individual clusters can contain up to six interpenetrating dendrimers. At about the dendrimer overlap density, $(4\pi\rho R_g^3)/3 \cong 1$, these clusters form crystal structures.

Spontaneous crystallization would be a slow and CPU-demanding process. On these grounds, we examined the stability of artificially constructed BCC and FCC cluster crystals for various densities with constant cluster size and found a region where such crystals remain mechanically stable. Within this stable region, the optimal cluster size and lattice constant were determined as function of the overall density by means of thermodynamic integration. The results showed that, on increasing the density, the average equilibrium cluster size grows, while the lattice constant decreases. The latter is different from the $Q^{\pm}$ models, where the lattice spacing of the cluster crystal remains density-independent, and is due to the fact that the effective pair-interaction is density dependent. In addition it was found that the FCC crystals are thermodynamically more stable than the BCC crystals.

We have restricted the free energy computations to BCC and FCC crystals only, which are considered to be the most likely candidates, as indicated from arguments based on density-functional considerations in the effective interaction picture.[29] Hence, it is possible that a different type of crystal arrangement might have an even lower free energy. In addition, we also restricted ourselves to cluster crystals with an integer cluster size. Since crystals appear to be stable with respect to various defects, it is plausible that at any given density the stable crystal will be formed with a narrow cluster size distribution, rather than a coexistence between two intertwined crystals with a different, perfect occupation numbers. This is also supported by a large similarity between the internal dendrimer and cluster structures, as evidenced by various density profiles, which suggest an insensitivity with respect to small local distortions or inhomogeneities.

The theoretical description of soft cluster crystals of macromolecules, based on the effective pair interaction in the infinite dilution limit, yields reliable predictions on the ranges of the thermodynamic parameters for which cluster crystals can be found, although the precise values are influenced by contributions beyond the pair-potential approximation. In the case of Model II, the density at freezing is underestimated

Reuse of AIP Publishing content is subject to the terms: https://publishing.aip.org/authors/rights-and-permissions. Downloaded to IP: 91.115.166.109 On: Mon, 23 May 2016 16:29:26

significantly. It was predicted to be found at $\rho_\times R_g^3 = 0.133$, but even at the Kirkwood instability $\rho_\lambda R_g^3 = 0.198$ of an absolutely unstable liquid phase, neither the BCC nor FCC cluster crystals could be mechanically stabilized. Although the actual coexisting densities between fluid and crystal have not been determined, the density of the least dense stable crystal is estimated to exceed the value $\rho_\times$ from MFA by about 60%. We have refrained from performing a free energy calculation of the fluid phase, since there is ample evidence that there is a regime in which crystals do not melt in the simulation, indicating their stability against the (cluster) fluid. Also the number of dendrimers per cluster is underestimated in the MFA and is actually found in the microscopic simulations to be twice as large. That said, the lowest cluster occupancies required to stabilize any crystal was only four dendrimers.

The clusters that form the building blocks of the crystal are well defined and easily identified due to the localization of the centers of mass of the dendrimers in a small spherical region with a radius of approximately half that of the radius of gyration of a single dendrimer. Whereas in an isolated dendrimer shell monomers can fold back into the core region, this is no longer the case once they are located in a cluster of several dendrimers. The solvophobic nature of the core-monomers results in a dense region that is well separated from all the surrounding shell monomers. The shell-monomers are less localized and can, depending on the overall density and occupation number, be found in a broad fairly homogeneous spherical shell or a double layer structure. The size of the individual dendrimers measured by means of their radius of gyration increases with decreasing density or increasing occupation number in the various mechanically stable crystals. It is an intriguing finding that in the optimal BCC and FCC cluster crystals, the radius of gyration of the Model II dendrimers is within 1% identical to that of an isolated dendrimer.

Given the limitations of the effective pair-potential approach and the importance of the monomer-resolved detail, it is natural to pose the question of what happens at densities even higher densities than the ones discussed here. In the range $\rho R_g^3 \gtrsim 0.6$, BCC cluster crystals could not be stabilized, but formed percolating structures of clusters. The thermodynamic integration results indicate that the free energies of the BCC and FCC crystals will be very close and hence like-wise also the FCC phase might become unstable. One possibility would be the formation of a different type of cluster crystal, but another possibility would be the formation of lamellar or bicontinuous structures by the core and shell monomers, which would be a 3D analog for results found by Malescio and Pellicane.[52] This problem, however, falls outside the scope of the current manuscript and is left for future work.

ACKNOWLEDGMENTS

We wish to thank Daan Frenkel (Cambridge University) for helpful discussions and Marta Montes-Saralegui for bringing up to our attention an erroneous result in a previous work,[43] which, however, has no consequences on the validity of the findings there and in the work at hand. D.A.L. thanks the Wolfgang Pauli Institute (WPI) for financial support. B.M.M. acknowledges the MFPL VIPS program (funded by BMWF and the City of Vienna), and EU funding (FP7-PEOPLE CIG-2011 No. 303860). Partial support by the Marie Curie ITN-COMPLOIDS (Grant Agreement No. 234810) and computer time at the Vienna Scientific Cluster (VSC) are gratefully acknowledged.

[1]D. Frenkel, Nature **440**, 4 (2006).
[2]B. M. Mladek, D. Gottwald, G. Kahl, M. Neumann, and C. N. Likos, Phys. Rev. Lett. **96**, 045701 (2006).
[3]F. Sciortino, S. Mossa, E. Zaccarelli, and P. Tartaglia, Phys. Rev. Lett. **93**, 55701 (2004).
[4]B. M. Mladek, D. Gottwald, G. Kahl, M. Neumann, and C. N. Likos, J. Phys. Chem. B **111**, 12799 (2007).
[5]S. D. Overduin and C. N. Likos, J. Chem. Phys. **131**, 034902 (2009).
[6]D. Coslovich, L. Strauss, and G. Kahl, Soft Matter **7**, 2127 (2011).
[7]D. A. Lenz, B. M. Mladek, C. N. Likos, G. Kahl, and R. Blaak, J. Phys. Chem. B **115**, 7218 (2011).
[8]D. Coslovich, M. Bernabei, and A. J. Moreno, J. Chem. Phys. **137**, 184904 (2012).
[9]M. Montes-Saralegui, A. Nikoubashman, and G. Kahl, J. Chem. Phys. **141**, 124908 (2014).
[10]N. B. Wilding and P. Sollich, J. Chem. Phys. **141**, 094903 (2014).
[11]N. Grewe and W. Klein, J. Math. Phys. **64**, 1729 (1977).
[12]N. Grewe and W. Klein, J. Math. Phys. **64**, 1735 (1977).
[13]W. Klein and N. Grewe, J. Chem. Phys. **72**, 5456 (1980).
[14]W. Klein and A. C. Brown, J. Chem. Phys. **74**, 6960 (1981).
[15]W. Klein, H. Gould, R. A. Ramos, I. Clejan, and A. I. Mel'cuk, Physica A **205**, 738 (1994).
[16]C. Marquest and T. A. Witten, J. Phys. (Paris) **50**, 1267 (1989).
[17]C. N. Likos, M. Watzlawek, and H. Löwen, Phys. Rev. E **58**, 3135 (1998).
[18]B. M. Mladek, G. Kahl, and C. N. Likos, Phys. Rev. Lett. **100**, 028301 (2008).
[19]C. N. Likos, A. Lang, M. Watzlawek, and H. Löwen, Phys. Rev. E **63**, 031206 (2001).
[20]B. M. Mladek, P. Charbonneau, and D. Frenkel, Phys. Rev. Lett. **99**, 235702 (2007).
[21]K. Zhang, P. Charbonneau, and B. M. Mladek, Phys. Rev. Lett. **105**, 245701 (2010).
[22]T. Neuhaus and C. N. Likos, J. Phys.: Condens. Matter **23**, 234112 (2011).
[23]A. J. Moreno and C. N. Likos, Phys. Rev. Lett. **99**, 107801 (2007).
[24]M. Montes-Saralegui, A. Nikoubashman, and G. Kahl, J. Phys.: Condens. Matter **25**, 195101 (2013).
[25]A. Nikoubashman, G. Kahl, and C. N. Likos, Phys. Rev. Lett. **107**, 068302 (2011).
[26]A. Nikoubashman, G. Kahl, and C. N. Likos, Soft Matter **8**, 4121 (2012).
[27]F. H. Stillinger and D. K. Stillinger, Physica A **244**, 358 (1997).
[28]A. Lang, C. N. Likos, M. Watzlawek, and H. Löwen, J. Phys.: Condens. Matter **12**, 5087 (2000).
[29]C. N. Likos, B. M. Mladek, D. Gottwald, and G. Kahl, J. Chem. Phys. **126**, 224502 (2007).
[30]A. Sütő, Commun. Math. Phys. **305**, 657 (2011).
[31]M. Ballauff and C. N. Likos, Angew. Chem., Int. Ed. **116**, 3060 (2004).
[32]I. O. Götze, H. M. Harreis, and C. N. Likos, J. Chem. Phys. **120**, 7761 (2004).
[33]A. A. Louis, P. G. Bolhuis, J. P. Hansen, and E. J. Meijer, Phys. Rev. Lett. **85**, 2522 (2000).
[34]A. Narros, A. J. Moreno, and C. N. Likos, Soft Matter **6**, 2435 (2010).
[35]C. Pierleoni, C. Addison, J. Hansen, and V. Krakoviack, Phys. Rev. Lett. **96**, 128302 (2006).
[36]J. Dautenhahn and C. K. Hall, Macromolecules **27**, 5399 (1994).
[37]C. N. Likos, Phys. Rep. **348**, 267 (2001).
[38]A. Narros, C. N. Likos, A. J. Moreno, and B. Capone, Soft Matter **10**, 9601 (2014).
[39]D. A. Lenz, R. Blaak, C. N. Likos, and B. M. Mladek, Phys. Rev. Lett. **109**, 228301 (2012).
[40]D. A. Lenz, R. Blaak, and C. N. Likos, Soft Matter **5**, 2905 (2009).
[41]D. A. Lenz, R. Blaak, and C. N. Likos, Soft Matter **5**, 4542 (2009).
[42]P. Welch and M. Muthukumar, Macromolecules **31**, 5892 (1998).
[43]After publication of Ref. 39, it was pointed out to us by Marta Montes-Saralegui that a mistake had been made in the computation of the effective pair-interaction for Model II, and consequently some derived numbers were incorrect. Fig. 2 shows the correct result. This error only affects, slightly, the numerical value of the predicted densities for the phase transition and lattice properties. All simulation results, however, were performed on the monomeric level and hence no other results of Ref. 39 are affected.

Reuse of AIP Publishing content is subject to the terms: https://publishing.aip.org/authors/rights-and-permissions. Downloaded to IP: 91.115.166.109 On: Mon, 23 May 2016 16:29:26

[44]D. Ruelle, *Statistical Mechanics* (Benjamin, New York, 1969).
[45]A. A. Louis, P. G. Bolhuis, and J.-P. Hansen, Phys. Rev. E **62** (2000).
[46]J. Hansen and I. R. McDonald, *Theory of Simple Liquids*, 3rd ed. (Academic Press, 2006).
[47]D. Frenkel and B. Smit, *Understanding Molecular Simulation*, 2nd ed. (Academic Press, London, 2002).
[48]D. Frenkel and A. J. C. Ladd, J. Chem. Phys. **81**, 3188 (1984).
[49]B. M. Mladek, P. Charbonneau, C. N. Likos, D. Frenkel, and G. Kahl, J. Phys.: Condens. Matter **20**, 494245 (2008).
[50]As a technical note, we like to mention that for $\lambda = 0$ the evaluation of the integrand in Eq. (10) does depend on the location of the origin of the crystal lattice within the simulation box. The unconstrained system obviously should not depend on this and its crystal positions would slowly diffuse throughout the simulation box. Such behavior is unwanted as it would produce large statistical fluctuations in the value of $\Phi - \Phi_{\mathrm{ref}}$ and very long simulation runs would be required in order to obtain the correct value. This problem can easily be overcome by introducing for the case $\lambda = 0$ random displacements of the origin of the lattice with an acceptance ratio of 100%, which effectively speeds up this diffusion process. For $\lambda \neq 0$ the drift of the center of mass of the full system is eliminated in a natural fashion and hence this additional type of Monte Carlo move is not required.[49]
[51]N. B. Wilding and P. Sollich, Europhys. Lett. **101**, 10004 (2013).
[52]G. Malescio and G. Pellicane, Phys. Rev. E **70**, 021202 (2004).

Reuse of AIP Publishing content is subject to the terms: https://publishing.aip.org/authors/rights-and-permissions. Downloaded to IP: 91.115.166.109 On: Mon, 23 May 2016 16:29:26